

AD-770 619

LASER MAN VERSUS MAN WEAPON FIRE
SIMULATION

Albert H. Marshall

Naval Training Equipment Center
Orlando, Florida

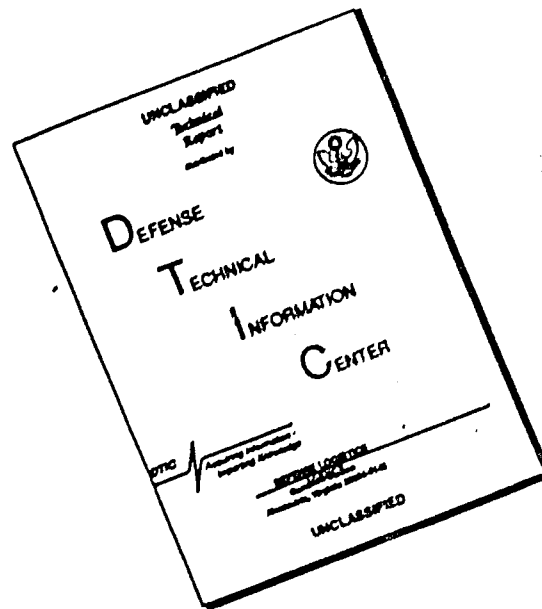
November 1973

DISTRIBUTED BY:

NTIS

National Technical Information Service
U. S. DEPARTMENT OF COMMERCE
5285 Port Royal Road, Springfield Va. 22151

DISCLAIMER NOTICE



THIS DOCUMENT IS BEST QUALITY AVAILABLE. THE COPY FURNISHED TO DTIC CONTAINED A SIGNIFICANT NUMBER OF PAGES WHICH DO NOT REPRODUCE LEGIBLY.

Unclassified
Security Classification

AD-770619

DOCUMENT CONTROL DATA - R & D

(Security classification of title, body of abstract and indexing annotation must be entered when the overall report is classified)

1. ORIGINATING ACTIVITY (Corporate author) Naval Training Equipment Center Orlando, Florida 32813		2a. REPORT SECURITY CLASSIFICATION Unclassified	
3. REPORT TITLE LASER MAN VERSUS MAN WEAPON FIRE SIMULATION		2b. GROUP	
4. DESCRIPTIVE NOTES (Type of report and inclusive dates) Technical Report (1973)			
5. AUTHOR(S) (First name, middle initial, last name) Albert H. Marshall			
6. REPORT DATE November 1973		7a. TOTAL NO. OF PAGES 203	7b. NO. OF PAGES 0
8a. CONTRACT OR GRANT NO.		9a. ORIGINATOR'S REPORT NUMBER(S) NAVTRAEQUIPCEN IH-227	
b. PROJECT NO. Task 3852		9b. OTHER REPORT NO(S) (Any other numbers that may be assigned this report)	
c.			
d.			
10. DISTRIBUTION STATEMENT Approved for public release; distribution unlimited			
11. SUPPLEMENTARY NOTES		12. SPONSORING MILITARY ACTIVITY Naval Training Equipment Center Orlando, Florida 32813	
13. ABSTRACT This report describes a man versus man semiconductor laser weapon fire simulation system that eliminates the requirement that the trainee wear on his body numerous laser detectors that impede his motion and are subject to damage. The system utilizes retroreflective material and two transmitted eyesafe laser beams. The first beam, when reflected, ascertains a hit and the second broad beam communicates this data back to the man who is hit. Detectors on the helmet receive the hit information.			

Reproduced by
NATIONAL TECHNICAL
INFORMATION SERVICE
U S Department of Commerce
Springfield VA 22151

Unclassified

Security Classification

14 REF. NO.	LINK A		LINK B		LINK C	
	ROLE	WT	ROLE	WT	ROLE	WT
LASER Detector Retroreflective material Weapon Fire Simulation LASER Beam Training Device						

ia

Technical Report: NAVTRAEQUIPCEN IH-227

LASER MAN VERSUS MAN
WEAPON FIRE SIMULATION

ABSTRACT

This report describes a man versus man semiconductor laser weapon fire simulation system that eliminates the requirement that the trainee wear on his body numerous laser detectors that impede his motion and are subject to damage. The system utilizes retroreflective material and two transmitted eyesafe laser beams. The first beam, when reflected, ascertains a hit and the second broad beam communicates this data back to the man who is hit. Detectors on the helmet receive the hit information.

1. TITLE		
2. AUTHOR		
3. PERFORMING ORGANIZATION		
4. REPORT NUMBER		
5. DISTRIBUTION STATEMENT	<input checked="" type="checkbox"/> UNCLASSIFIED	
6. SUBJECT TERMS		
7. AUTHOR AVAILABILITY CODES		
8. DISTRIBUTION STATEMENT	<input type="checkbox"/> UNCLASSIFIED	
9. DISTRIBUTION STATEMENT	<input type="checkbox"/> UNCLASSIFIED	
10. DISTRIBUTION STATEMENT	<input type="checkbox"/> UNCLASSIFIED	
11. DISTRIBUTION STATEMENT	<input type="checkbox"/> UNCLASSIFIED	
12. DISTRIBUTION STATEMENT	<input type="checkbox"/> UNCLASSIFIED	
13. DISTRIBUTION STATEMENT	<input type="checkbox"/> UNCLASSIFIED	
14. DISTRIBUTION STATEMENT	<input type="checkbox"/> UNCLASSIFIED	
15. DISTRIBUTION STATEMENT	<input type="checkbox"/> UNCLASSIFIED	
16. DISTRIBUTION STATEMENT	<input type="checkbox"/> UNCLASSIFIED	
17. DISTRIBUTION STATEMENT	<input type="checkbox"/> UNCLASSIFIED	
18. DISTRIBUTION STATEMENT	<input type="checkbox"/> UNCLASSIFIED	
19. DISTRIBUTION STATEMENT	<input type="checkbox"/> UNCLASSIFIED	
20. DISTRIBUTION STATEMENT	<input type="checkbox"/> UNCLASSIFIED	
21. DISTRIBUTION STATEMENT	<input type="checkbox"/> UNCLASSIFIED	
22. DISTRIBUTION STATEMENT	<input type="checkbox"/> UNCLASSIFIED	
23. DISTRIBUTION STATEMENT	<input type="checkbox"/> UNCLASSIFIED	
24. DISTRIBUTION STATEMENT	<input type="checkbox"/> UNCLASSIFIED	
25. DISTRIBUTION STATEMENT	<input type="checkbox"/> UNCLASSIFIED	
26. DISTRIBUTION STATEMENT	<input type="checkbox"/> UNCLASSIFIED	
27. DISTRIBUTION STATEMENT	<input type="checkbox"/> UNCLASSIFIED	
28. DISTRIBUTION STATEMENT	<input type="checkbox"/> UNCLASSIFIED	
29. DISTRIBUTION STATEMENT	<input type="checkbox"/> UNCLASSIFIED	
30. DISTRIBUTION STATEMENT	<input type="checkbox"/> UNCLASSIFIED	
31. DISTRIBUTION STATEMENT	<input type="checkbox"/> UNCLASSIFIED	
32. DISTRIBUTION STATEMENT	<input type="checkbox"/> UNCLASSIFIED	
33. DISTRIBUTION STATEMENT	<input type="checkbox"/> UNCLASSIFIED	
34. DISTRIBUTION STATEMENT	<input type="checkbox"/> UNCLASSIFIED	
35. DISTRIBUTION STATEMENT	<input type="checkbox"/> UNCLASSIFIED	
36. DISTRIBUTION STATEMENT	<input type="checkbox"/> UNCLASSIFIED	
37. DISTRIBUTION STATEMENT	<input type="checkbox"/> UNCLASSIFIED	
38. DISTRIBUTION STATEMENT	<input type="checkbox"/> UNCLASSIFIED	
39. DISTRIBUTION STATEMENT	<input type="checkbox"/> UNCLASSIFIED	
40. DISTRIBUTION STATEMENT	<input type="checkbox"/> UNCLASSIFIED	
41. DISTRIBUTION STATEMENT	<input type="checkbox"/> UNCLASSIFIED	
42. DISTRIBUTION STATEMENT	<input type="checkbox"/> UNCLASSIFIED	
43. DISTRIBUTION STATEMENT	<input type="checkbox"/> UNCLASSIFIED	
44. DISTRIBUTION STATEMENT	<input type="checkbox"/> UNCLASSIFIED	
45. DISTRIBUTION STATEMENT	<input type="checkbox"/> UNCLASSIFIED	
46. DISTRIBUTION STATEMENT	<input type="checkbox"/> UNCLASSIFIED	
47. DISTRIBUTION STATEMENT	<input type="checkbox"/> UNCLASSIFIED	
48. DISTRIBUTION STATEMENT	<input type="checkbox"/> UNCLASSIFIED	
49. DISTRIBUTION STATEMENT	<input type="checkbox"/> UNCLASSIFIED	
50. DISTRIBUTION STATEMENT	<input type="checkbox"/> UNCLASSIFIED	
51. DISTRIBUTION STATEMENT	<input type="checkbox"/> UNCLASSIFIED	
52. DISTRIBUTION STATEMENT	<input type="checkbox"/> UNCLASSIFIED	
53. DISTRIBUTION STATEMENT	<input type="checkbox"/> UNCLASSIFIED	
54. DISTRIBUTION STATEMENT	<input type="checkbox"/> UNCLASSIFIED	
55. DISTRIBUTION STATEMENT	<input type="checkbox"/> UNCLASSIFIED	
56. DISTRIBUTION STATEMENT	<input type="checkbox"/> UNCLASSIFIED	
57. DISTRIBUTION STATEMENT	<input type="checkbox"/> UNCLASSIFIED	
58. DISTRIBUTION STATEMENT	<input type="checkbox"/> UNCLASSIFIED	
59. DISTRIBUTION STATEMENT	<input type="checkbox"/> UNCLASSIFIED	
60. DISTRIBUTION STATEMENT	<input type="checkbox"/> UNCLASSIFIED	
61. DISTRIBUTION STATEMENT	<input type="checkbox"/> UNCLASSIFIED	
62. DISTRIBUTION STATEMENT	<input type="checkbox"/> UNCLASSIFIED	
63. DISTRIBUTION STATEMENT	<input type="checkbox"/> UNCLASSIFIED	
64. DISTRIBUTION STATEMENT	<input type="checkbox"/> UNCLASSIFIED	
65. DISTRIBUTION STATEMENT	<input type="checkbox"/> UNCLASSIFIED	
66. DISTRIBUTION STATEMENT	<input type="checkbox"/> UNCLASSIFIED	
67. DISTRIBUTION STATEMENT	<input type="checkbox"/> UNCLASSIFIED	
68. DISTRIBUTION STATEMENT	<input type="checkbox"/> UNCLASSIFIED	
69. DISTRIBUTION STATEMENT	<input type="checkbox"/> UNCLASSIFIED	
70. DISTRIBUTION STATEMENT	<input type="checkbox"/> UNCLASSIFIED	
71. DISTRIBUTION STATEMENT	<input type="checkbox"/> UNCLASSIFIED	
72. DISTRIBUTION STATEMENT	<input type="checkbox"/> UNCLASSIFIED	
73. DISTRIBUTION STATEMENT	<input type="checkbox"/> UNCLASSIFIED	
74. DISTRIBUTION STATEMENT	<input type="checkbox"/> UNCLASSIFIED	
75. DISTRIBUTION STATEMENT	<input type="checkbox"/> UNCLASSIFIED	
76. DISTRIBUTION STATEMENT	<input type="checkbox"/> UNCLASSIFIED	
77. DISTRIBUTION STATEMENT	<input type="checkbox"/> UNCLASSIFIED	
78. DISTRIBUTION STATEMENT	<input type="checkbox"/> UNCLASSIFIED	
79. DISTRIBUTION STATEMENT	<input type="checkbox"/> UNCLASSIFIED	
80. DISTRIBUTION STATEMENT	<input type="checkbox"/> UNCLASSIFIED	
81. DISTRIBUTION STATEMENT	<input type="checkbox"/> UNCLASSIFIED	
82. DISTRIBUTION STATEMENT	<input type="checkbox"/> UNCLASSIFIED	
83. DISTRIBUTION STATEMENT	<input type="checkbox"/> UNCLASSIFIED	
84. DISTRIBUTION STATEMENT	<input type="checkbox"/> UNCLASSIFIED	
85. DISTRIBUTION STATEMENT	<input type="checkbox"/> UNCLASSIFIED	
86. DISTRIBUTION STATEMENT	<input type="checkbox"/> UNCLASSIFIED	
87. DISTRIBUTION STATEMENT	<input type="checkbox"/> UNCLASSIFIED	
88. DISTRIBUTION STATEMENT	<input type="checkbox"/> UNCLASSIFIED	
89. DISTRIBUTION STATEMENT	<input type="checkbox"/> UNCLASSIFIED	
90. DISTRIBUTION STATEMENT	<input type="checkbox"/> UNCLASSIFIED	
91. DISTRIBUTION STATEMENT	<input type="checkbox"/> UNCLASSIFIED	
92. DISTRIBUTION STATEMENT	<input type="checkbox"/> UNCLASSIFIED	
93. DISTRIBUTION STATEMENT	<input type="checkbox"/> UNCLASSIFIED	
94. DISTRIBUTION STATEMENT	<input type="checkbox"/> UNCLASSIFIED	
95. DISTRIBUTION STATEMENT	<input type="checkbox"/> UNCLASSIFIED	
96. DISTRIBUTION STATEMENT	<input type="checkbox"/> UNCLASSIFIED	
97. DISTRIBUTION STATEMENT	<input type="checkbox"/> UNCLASSIFIED	
98. DISTRIBUTION STATEMENT	<input type="checkbox"/> UNCLASSIFIED	
99. DISTRIBUTION STATEMENT	<input type="checkbox"/> UNCLASSIFIED	
100. DISTRIBUTION STATEMENT	<input type="checkbox"/> UNCLASSIFIED	

GOVERNMENT RIGHTS IN DATA STATEMENT

Reproduction of this publication in whole or in part is permitted for any purpose of the United States Government.

ih

NAVTRAEQUIPCEN IH-227


LASER MAN VERSUS MAN
WEAPON FIRE SIMULATION

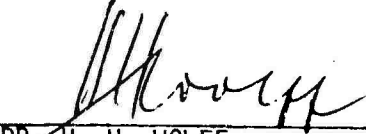
Albert H. Marshall

Physical Sciences Laboratory

November 1973

Approved:


GEORGE BERDERIAN
Head, Physical Sciences Laboratory


DR. H. H. WOLFF
Technical Director

NAVAL TRAINING EQUIPMENT CENTER
ORLANDO, FLORIDA

TABLE OF CONTENTS

<u>SECTION</u>		<u>PAGE</u>
I	INTRODUCTION	1
II	THEORY	5
	A. LASER RIFLE	5
	B. HELMET LASER RECEIVER	19
III	CONCLUSIONS AND RECOMMENDATIONS	23
	BIBLIOGRAPHY	24

LIST OF ILLUSTRATIONS

<u>Figure</u>		<u>Page</u>
1	Man Versus Man System	3
1A	Man Versus Man System	4
2	Effect of Reverse Bias on Detector Capacitance	8
3	Normalized Quantum Efficiency versus Wavelength	9
4	Functional Representation of an Avalanche Photodiode . . .	10
5	Signal Power and Noise Power versus Photocurrent Gain . . .	11
6	Photocurrent Gain versus Reverse Voltage.	11
7	Transimpedance Amplifier Schematic.	12
8	Optimum Gain versus Background Radiation	14
9	Laser Rifle Schematic	17
10	Integrated Circuit Timer	18
11	Helmet Laser Receiver	20

SECTION I

INTRODUCTION

This report describes a "man vs. man" weapon fire simulation which allows trainees to conduct realistic, safe war games.

Previous man-to-man combat simulation systems required the trainee to wear on his body numerous laser detectors which impeded his motion and were easily damaged when it was necessary for the trainee to crawl on the ground. Also, necessary equipment the trainee carried shielded some of the detectors and, as a consequence, some of the hits were not recorded.

This system also informs the trainee using the laser gun when he has scored a hit.

In this system, each man wears a reflective fabric vest or a training uniform sprayed with reflective paint which consists of microscopic glass spheres. The paint containing the glass spheres is marketed commercially and will retain its reflectivity after conventional washing, pressing or dry cleaning.

Each trainee is equipped with a special laser rifle which has two laser transmitters, one to produce a narrow beam to simulate the weapon's characteristics and a second to provide a broad beam to communicate back to the victim that he has been hit. An improved version will combine the laser transmitters into one system. The "communicating" broad beam laser eliminates the necessity of covering the man with detectors and also eliminates the need for using a radio to inform the man-target he has been hit. The detectors used to indicate a hit are located on the man's helmet. A unique four-detector system, with a 360° field of view, has been developed that works without expensive optical filters which are customarily required when training in bright sunlight conditions.

If the trainee's sights are properly aligned on his opponent when he squeezes the trigger, the narrow transmitter beam's single pulse of near infrared laser energy, which is not visible to the human eye, is reflected from the "reflective" uniform back to the laser rifle. An eyesafe Gallium Arsenide laser is used in both transmitters. The returned pulse is detected by a silicon avalanche photodiode detector located in the stock of the rifle. Signal current gain in the avalanche detector greatly improves the sensitivity of the laser receiver. If the detected pulse exceeds the threshold value on a voltage comparator in the receiver, the rifle performs three simultaneous operations.

° A light emitting diode, LED, indicator is turned on briefly on the weapon's sight. This tells the shooter immediately that he has scored a hit.

NAVTRAEQUIPCEN IH-227

°The hit is counted on a miniature counter in the underside of the rifle. This can later be read by an umpire using an external read-out box.

°The broad beam laser transmitter used to inform the victim he has been hit is pulsed.

The transmitted broad beam is detected on the hit victim by the four photodetectors located on the victim's helmet. This signal turns on an audible alarm, also located on the helmet. A visible marker can be utilized to replace or supplement the audio alarm. In order to turn off the alarm on his helmet, the hit victim must use a special key located in his rifle which, when removed, disables the rifle thus removing the hit trainee from the war game. Both laser beams are eyesafe.

The prototype equipment is shown in figure 1.



Figure 1. Man versus Man System



Figure 1A. Man versus Man System

SECTION II

THEORY

A. LASER RIFLE

The rifle bullet is simulated by a pulse of laser infrared energy transmitted by a semiconductor, gallium arsenide laser. A single pulse is transmitted when the trigger is pulled.

A gallium arsenide laser is a p-n diode in which a fraction of the injected minority carriers recombine by means of radiative transitions. The semiconductor laser is basically a planar p-n junction in a single crystal of gallium arsenide. Two of the parallel semireflective faces form a Fabry-Perot resonant cavity that enhances the optical Q of the system. The radiant flux is emitted from the thin rectangular area of the junction. The junction dimensions are determined by the semiconductor chip size; the longer dimension varies as a function of the chip size and the smaller dimension is determined by the carrier-diffusion distance, which is 2 μm in GaAs by doping level and junction configuration. The emitting region is 6X0.08 Mils.

This laser emits coherent radiation in the near IR region at 904 nm (27°C) with a spectral bandwidth of 1 nm. The wavelength changes 0.23 nm/°C with increasing or decreasing temperature.

The laser diode used has a five watt peak power pulse in a 180 n.sec pulse width.

The laser is driven with a 20 ampere current pulse. The current pulse is generated by a transistor pulser circuit.

The laser diode radiation pattern in the plane perpendicular to the plane at the junction is 20° at the half radiant intensity points and approximately 10° in the plane at the junction. The transmitter beam is collimated using a simple double convex lens with a 37.5 mm focal length, f#1.5. To obtain the maximum energy collection, it is necessary to use a low f number lens. To obtain the minimum beam divergence, a long focal length lens is required. This selection of lens represents a compromise between maximum power and minimum beam divergence.

If the trainee is properly sighted on the target, the transmitted laser beam is retroreflected from microscopic glass beads sprayed on the uniform or pack of the trainee. The reflectivity of the sprayed material is 100 times that of flat white paint.

The reflected narrow beam used to simulate the bullet is detected by a silicon avalanche photodiode. Previous techniques and devices for accomplishing laser detection requirements include the photomultiplier, photoconductive detectors and reverse biased P-I-N photodiodes. The photomultiplier tube until the recent development of avalanche photodiodes

most nearly meets these requirements; however, since the gallium arsenide, semiconductor laser operates at 904 nm at room temperature or in the near infrared, the photomultipliers quantum efficiency is quite low. Detectors utilizing the photoconductive effect are not suitable because they are limited at present to frequencies below the microwave range and are narrow band devices. The P-I-N photodiode is suitable for detection of these pulses but they have no inherent gain and are thermal noise limited. Avalanche photodiodes can provide gain and are best suited for low-level detection of Gallium-Arsenide laser pulses.

The avalanche photodiode is especially suited for low-noise application where the principal noise source is the preamplifier. Avalanche photodiodes have characteristics similar to a conventional photodiode with the addition of an internal linear current-gain mechanism due to the avalanche effect. The gain is determined by the applied reverse bias which is just below the breakdown voltage of the diode. Signal current gain in avalanche detectors greatly improves the sensitivity of the laser receiver.

The avalanche breakdown effect is similar to the Townsend discharge in gas filled tubes and relies on the ionization of carriers on impact collision of atoms by other carriers which have been imparted sufficient energy by an electric field. If a free electron and hole is created by an absorbed photon within the depletion layer of the diode junction, and an electric field is applied, the carriers will increase their velocity and kinetic energy in the direction of the electric field. As the carriers move in the lattice structure inside the semiconductor, the free carrier may collide with an atom within the junction and, because of their high energy level they can rip off additional carriers from the atom. The free carriers essentially "kick" new electrons from the valence to the conduction band, while still transversing the depletion layer. Providing sufficient energy still remains in the original colliding carrier, additional collisions and thus other carriers will be freed from additional atoms. The newly released carriers now gain sufficient energy from the field to begin collisions of their own. Thus, multiplication of the carriers has occurred and its degree is a function of how near to the breakdown voltage the diode is biased.

Two types of breakdown can occur in diodes. In narrow p-n junctions an effect known as field emission was described by Zener in 1934. Zener's original theory was that under very intense electric fields (10^5 V/cm or greater), electrons are pulled out of the valence band and traverse the forbidden energy gap by quantum-mechanical tunneling. In avalanche diodes, with wider junctions, the newer theory of avalanche breakdown must be utilized.

In avalanche breakdown the junction does not suddenly begin to conduct very large currents all over the junction but rather at small discrete points. These small high-current-density discharges are called microplasmas. Microplasmas occur preferentially along areas of lattice damage at the junction [1].

An avalanche detector consists of a deep-diffused graded p-n junction in a silicon wafer. This type of diode is fabricated by diffusion of gallium into high resistivity n-type silicon. Quality of the silicon is of great importance because fluctuations in the doping (striations) can cause large variations in the electric field distribution and therefore, to large changes in avalanche gain over the sensitive area. Dislocations and other lattice defects cause premature avalanche breakdown in "micro-plasmas" and render the device useless at this point because of the high noise current [2]. Recent advances in the growth of high resistivity, very uniformly doped silicon and careful processing techniques have resulted in high quantum efficiencies and very large avalanche gains. Surface breakdown is avoided by "contouring", which limits the surface field to values far below that in the interior of the diode. Contouring minimizes the surface leakage current and permits very large reverse voltages across the junction without surface breakdown.

As reverse bias is applied to the detector, the space charge region begins to build up, and an effective capacitance appears across this region. The capacitance is analogous to a parallel plate capacitor whose plates correspond to the space charge region boundary, filled with a dielectric whose dielectric constant is that of silicon. As the detector bias is increased, the space charge region becomes thicker, and the capacitance decreases, since it is inversely proportional to the thickness.

Capacitance of the diode depletion region can be calculated from

$$C = \frac{\epsilon A}{x_2 - x_1}$$

where

ϵ = permittivity of semiconductor material,

A = area of avalanche diode,

$x_2 - x_1$ = thickness of active region.

Due to the dimensions of the avalanche photodiode the frequency response is limited by the transient-time effects and not by the RC cutoff. The avalanche detector used has a capacitance of 8 pf. near avalanche. Figure 2 illustrates how the capacitance varies as a function of the applied reverse bias voltage. [3].

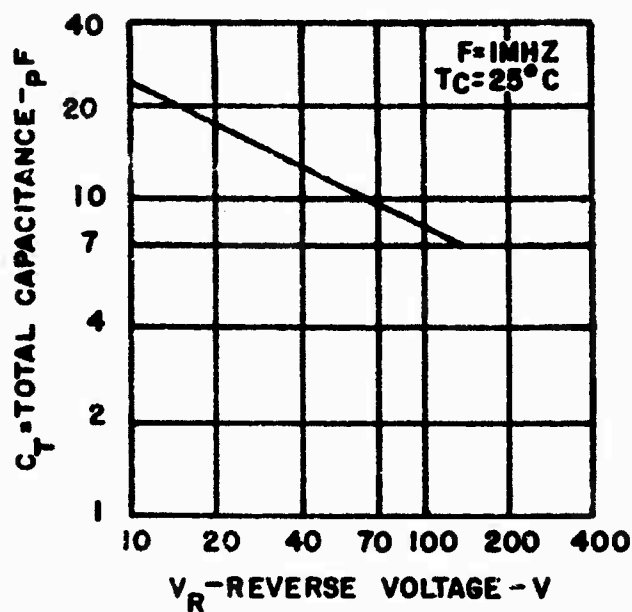


Figure 2. Effect of Reverse Bias on Detector Capacitance

When a photon enters the detector, the internal quantum efficiency is based on Lambert's Law. This law states that when light enters any thin layer of material perpendicular to the direction of propagation, the intensity is reduced proportional to the thickness of the layer. The photon flux after having penetrated the detector to a distance X is:

$$\bar{\Phi}(x) = \bar{\Phi}_0 e^{-\alpha x}$$

where

$\bar{\Phi}$ = photon flux incident on the detector,

α = absorption coefficient.

This formulation neglects both front-surface and internal reflections. Assuming each photon absorbed generates a hole-electron pair the quantum efficiency η , is

$$\eta = 1 - e^{-\alpha x_m}$$

The quantum efficiency of the avalanche detector is 70 percent at 0.9 microns.

The quantum efficiency varies as a function of the wavelength of the incident radiation. Silicon has an excellent quantum efficiency at the frequency of GaAs lasers (0.9 μm at 25°C). A plot of the normalized quantum efficiency versus wavelength is shown in figure 3.

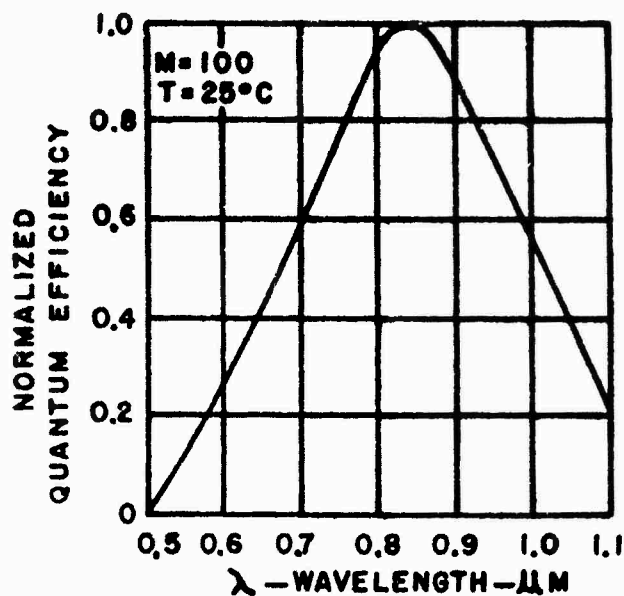


Figure 3. Normalized Quantum Efficiency vs. Wavelength

Functionally the avalanche detector can be thought of as a p-type region which acts to collect the charge, followed by a variable (0 to 80 nanosec.) delay line. The n-type region can be considered a preamplifier with a gain figure, proportional to avalanche multiplication, M . A functional representation of the detector is shown in figure 4.

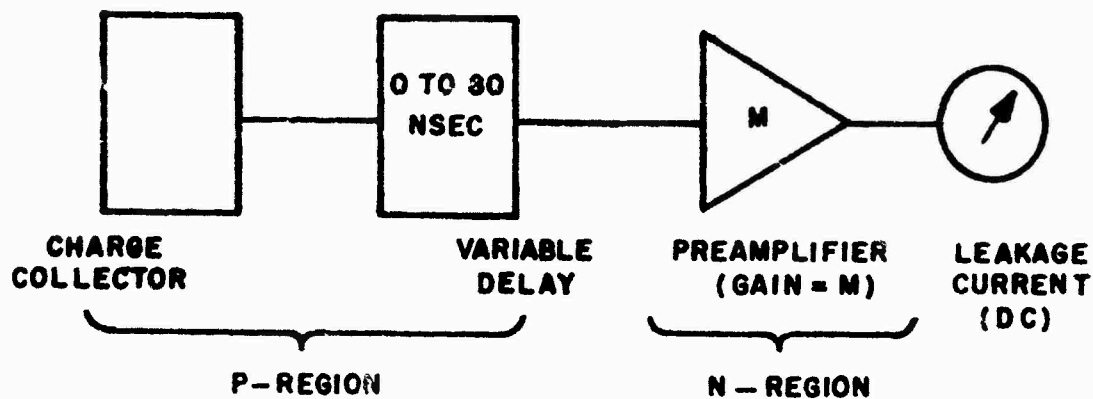


Figure 4. Functional Representation of an Avalanche Photodiode.

Multiplication by a factor M of the avalanche diodes photocurrent leads to an increase of M^2 of the signal power over the power which is normally available from a conventional photodiode. This effect is similar to that of the signal power from a photomultiplier, however, in this case, the avalanche gain M plays the role of the secondary electron multiplication gain. However, a problem arises because as shown in figure 5, the noise does not increase as M^2 , but as $M^{2.3}$. Photocurrent gain versus reverse detector bias is shown in figure 6. A theoretical study performed by McIntyre [4] predicted that if the multiplication is due to either holes or electrons then the multiplication factor of the signal power is M^2 .

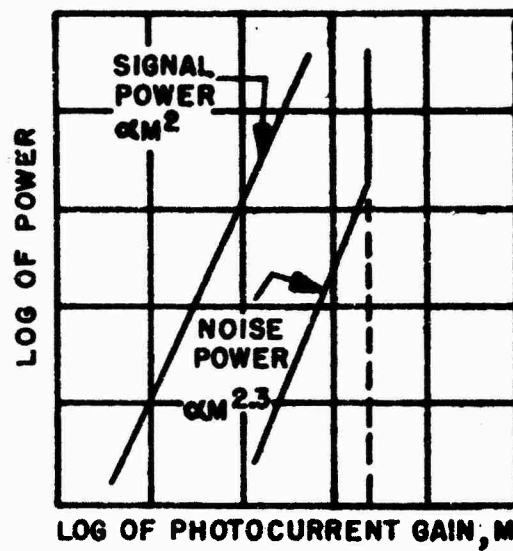


Figure 5. Signal Power and Noise Power versus Photocurrent Gain

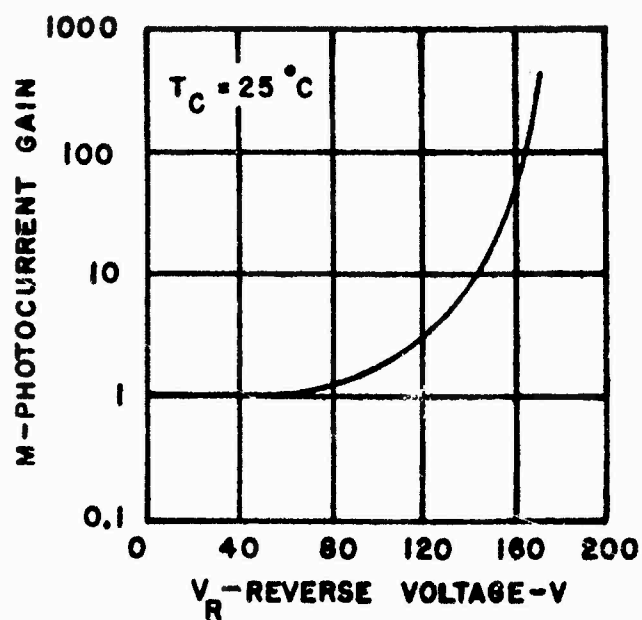


Figure 6. Photocurrent Gain versus Reverse Detector Bias

If both holes and electrons are equally effective in producing electron-hole pairs, then $M^{2.3}$ applies for this detector.

The ability to detect optical pulses with the avalanche detector is limited in accuracy by random fluctuations called noise. Three types of noise determine the minimum detectable signal in an optical receiver. The first is noise generated in the detector by the dark current. This noise increases dramatically at the breakdown voltage. The second type noise is induced by the recombination noise and is attributed to the random way in which electrons are generated in the detector.

In conventional photodiode receivers, the amplifier noise dominates, except for receivers having wide field of views, where the photon shot noise generated by the background can become larger than the amplifier noise. The dark noise of an avalanche detector is much smaller than the amplifier noise.

The avalanche photodiode is a high-impedance device, and for moderate values of avalanche gain, the equivalent parallel resistance of the diode is large compared to the normal circuit impedances. Therefore, the avalanche detector is a current source and the equivalent input noise current is the most useful parameter for describing the second-stage amplifier noise. The detector output goes to a low-noise high-speed transimpedance amplifier designed for current sources. The amplifier provides an output voltage which is linearly proportional to the detector's input current. A schematic of the amplifier and diode detector is shown in figure 7.

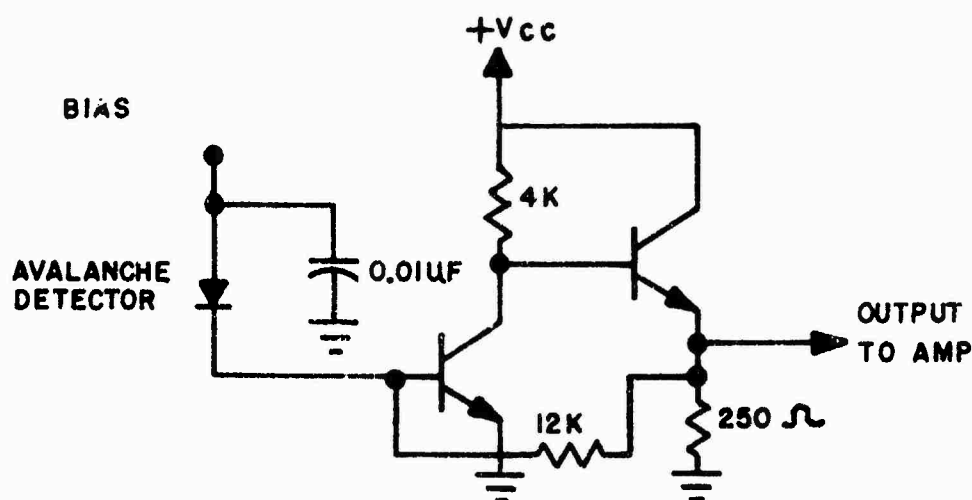


Figure 7. Schematic of Amplifier and Diode Detector

The input noise current of the amplifier is $i_x = 3 \times 10^{-12} \text{ A}/\sqrt{\text{Hz}}$.

With a load resistance of 50 ohms the (-3dB) bandwidth is 18 MHz.

The responsivity, R_o are 0.5 Amperes/Watt at $0.9 \mu\text{m}$ ($M=1$). M is the multiplication factor which is 100 maximum. When the detector is not background limited one can determine the value of the noise equivalent power (NEP) of an avalanche receiver system. The amplifier noise can be expressed as a spectral noise current density, i'_x , referred to the input of the amplifier, and its dimensions are $\text{A}/\sqrt{\text{Hz}}$. NEP is then defined as

$$\text{NEP} = \frac{i_x}{R_o M} = \frac{3 \times 10^{-12} \text{ A}/\sqrt{\text{Hz}}}{0.5 \text{ A/W} \times 100} = 6 \times 10^{-14} \text{ W}/\sqrt{\text{Hz}} \quad (\text{at } 0.9 \mu\text{m})$$

Therefore, in the absence of background, the combined diode and amplifier noise equivalent power is $6 \times 10^{-14} \text{ W}/\sqrt{\text{Hz}}$.

The avalanche gain necessary for optimum signal to noise operation in the presence of background radiation incident on the detector will be determined next. Signal current, i'_s , from the avalanche detector is given by, $i'_s = P_{\text{rcvd}} R_o M$ where P_{rcvd} is the received laser signal power. The noise, i'_n , is the sum of the dark noise and the noise current due to background radiation, P_{bgr} on the detector. The background noise is represented by $i'_{\text{bgr}} = P_{\text{bgr}} R_o$. McIntyre's theory [4] states the system noise, i'_n , is multiplied at a higher power than the signal power, or $M^{2.3}$. Accordingly, the noise current can be expressed as $i'_n = [2q(i_d + i_{\text{bgr}})M^{2.3} \Delta f]^{1/2}$ where i_d is the dark current at $M=1$, q is the charge of an electron and Δf is the receiver bandwidth.

Signal-to-noise power ratio is given by

$$\left(\frac{i_s}{i_n}\right)^2 = \frac{(P_{revd} R_o M)^2}{[2q(i_d + i_{bgr}) M^{2.3} \Delta f]}$$

The amplifier noise is given by $i_x^2 \Delta f$. Accounting for amplifier noise the signal-to-noise ratio for the receiver is

$$\left(\frac{i_s}{i_n}\right)^2 = \frac{P_{revd}^2 R_o^2 M^2}{[2q(i_d + P_{bgr} R_o) M^{2.3} + i_x^2] \Delta f}$$

Note that because $M^{2.3}$ occurs in the denominator; the denominator grows faster than the numerator and M is therefore limited as a function of P_{bgr} . The optimum operating M is obtained when $\left(\frac{i_s}{i_n}\right)^2$ is a maximum. Multiplication gain at this condition is given by

$$M_{opt} = \left[\frac{i_x^2}{(2.3-2)q(i_d + R_o P_{bgr})} \right]^{\frac{1}{2.3}}$$

Dark current is given by $i_d = 25 \times 10^{-12}$ amp.

Figure 8 is a plot of optimum gain versus background radiation.

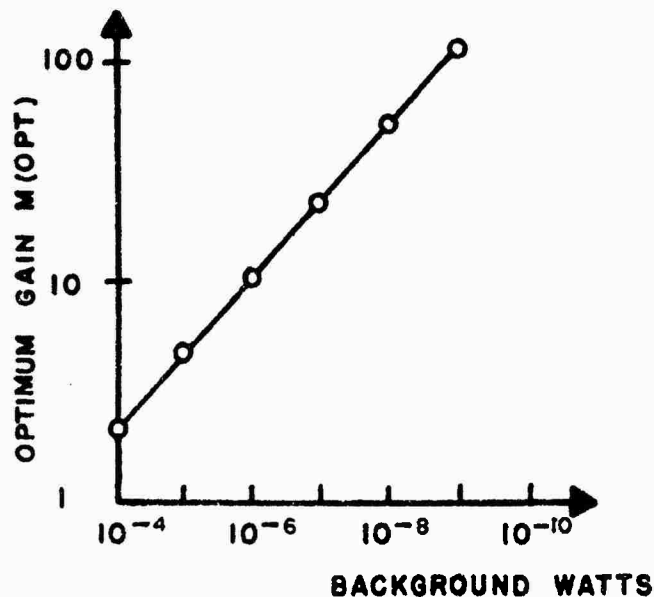


Figure 8. Optimum Gain, $M(opt)$, versus Background Radiation

Effects of optical background radiation are minimized by utilizing a narrow band optical interference filter in front of the detector optics and also a narrow field of view optical system for the receiver optics. These devices reduce the background noise and permit a greater detector gain, M.

The power received from a reflected laser beam, P_{rec} can be expressed using the following equation,^[5] for laser range finders

$$P_{rec} = \frac{P_t T_t \rho \cos \theta A_r T_r}{\pi R^2} \exp(-2\sigma R)$$

In this equation the two-way path transmittance loss through the atmosphere is given by $\exp(-2\sigma R)$, and

P_t = peak transmitted laser power (watts)

T_t = transmittance of laser optics

R = range (m)

$\rho \cos \theta$ = target reflectance as a function of the angle of beam incidence to the target surface

A_r = collecting area of receiver optics (m^2)

T_r = transmittance of receiver optics

Note that the power received can be increased by increasing the diameter of the collecting optical area. The receiver lens must also limit the field of view so a maximum M is realized. However, the field of view of the receiver optics should not be smaller than the laser beam on the target. The background power is given by

$$P_{bg} = \frac{H_{\lambda s} B_o \alpha_r^2 A_r T_r}{4} \rho \exp(-\sigma R)$$

where

$H_{\lambda s}$ = solar spectral irradiance ($Wm^{-2}\text{\AA}^{-1}$) at a given wavelength

B_o = pass band at the optical receiver

α_r = receiver beamwidth (rad)

A_r = collection area of receiver optics

T_r = transmittance of receiver optics

ρ = target reflectance

NAVTRALQUIPCEN III-227

This equation assumes complete blocking except for the optical filter passband and ignores atmospheric backscattering. The background, P_{gr} can be seen to decrease as B_0 , the filter bandwidth, is made narrower. A 15 nm filter with 70 percent transmissions is utilized in the system. A narrower interference filter could have been used in the receiver, but since the laser drifts .23 nm/°C, the 15 nm filter was employed.

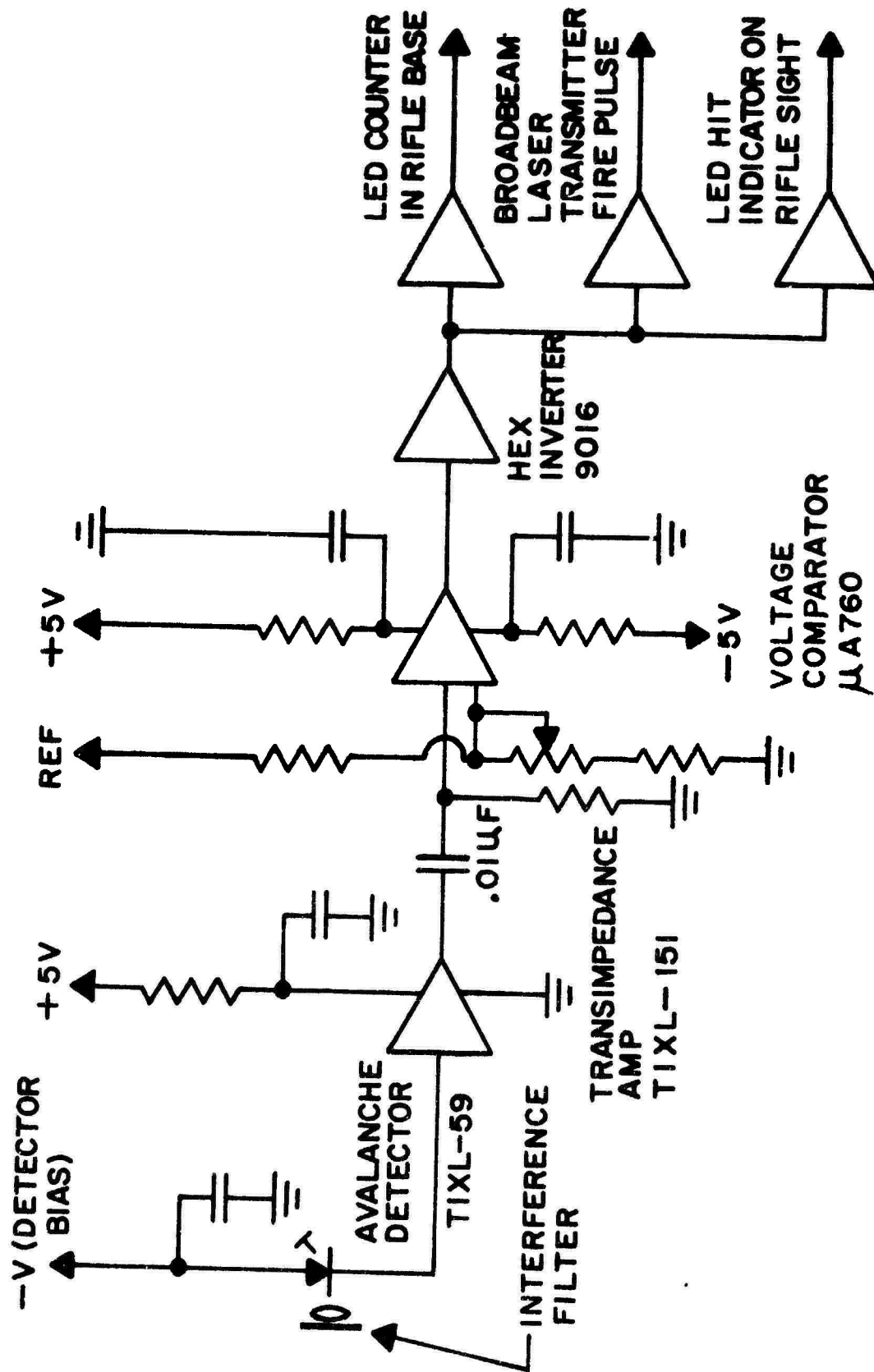


Figure 9. Rifle Schematic

The laser rifle schematic is shown in figure 9. Output from the transimpedance amplifier shown in figure 7 is fed to a high-speed voltage comparator. The voltage comparator is used to accomplish level detection of the input signal with a known reference level. When the input signal exceeds the established reference limit, the comparator output changes states. Typical response times for the comparator is 18 ns. Output from the voltage comparator is utilized to drive a Hex Inverter. Inverter outputs accomplish the following:

- ° Record a "kill" count on the LED counter in the base of the rifle.
- ° Fire the broad "communicating" beam laser transmitter, used to inform the victim he has been hit.
- ° Briefly turn on a LED on the sight to inform the trainee he has scored a kill.

The LED on the sight is turned on and off by a small integrated circuit timer, shown in figure 10. Times can be selected by a resistor and capacitor.

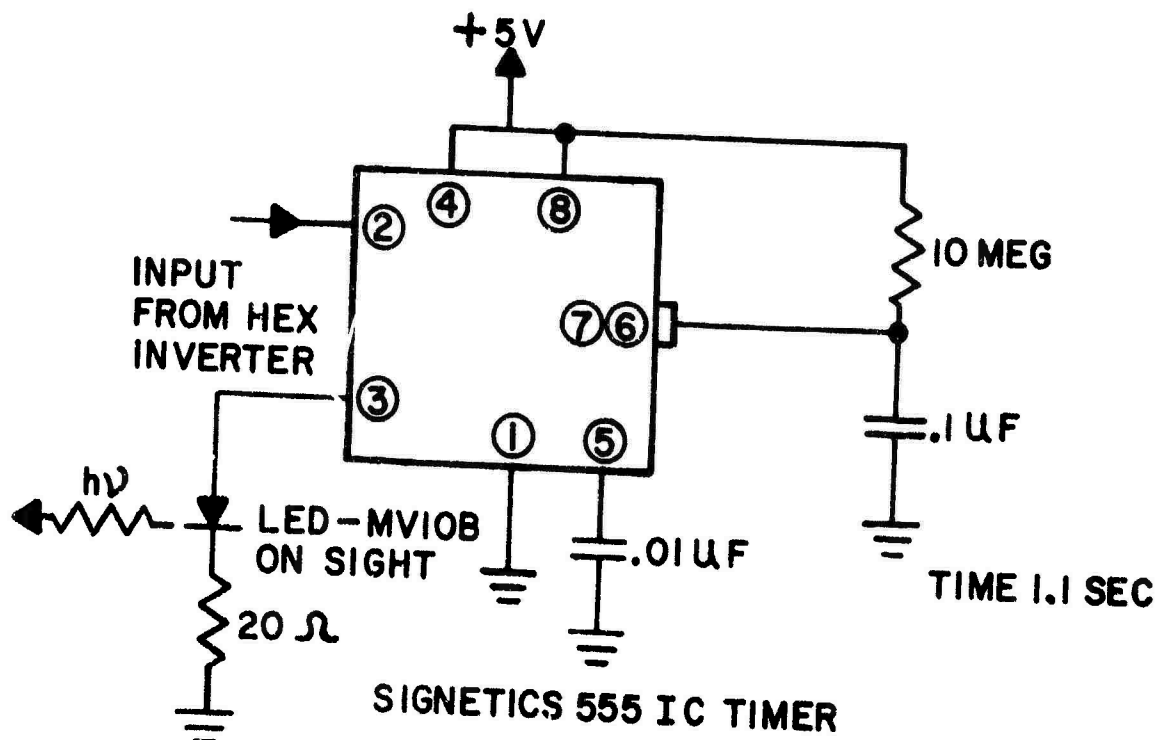


Figure 10. Integrated Circuit Timer

B. HELMET LASER RECEIVER

Four silicon photodiode detectors are located on the helmet of the trainee to detect the signal transmitted from the laser rifle by the large elliptical laser beam. The larger laser beam is used to communicate to the victim he has been hit and is fired only if the first transmitted narrow beam is on the retroreflective target.

The number of detectors on the helmet can be reduced from four if a prism or optical fibers are utilized.

Detectors located on the helmet can be well protected and are far less susceptible to field damage. The helmet laser receiver is shown in figure 11.

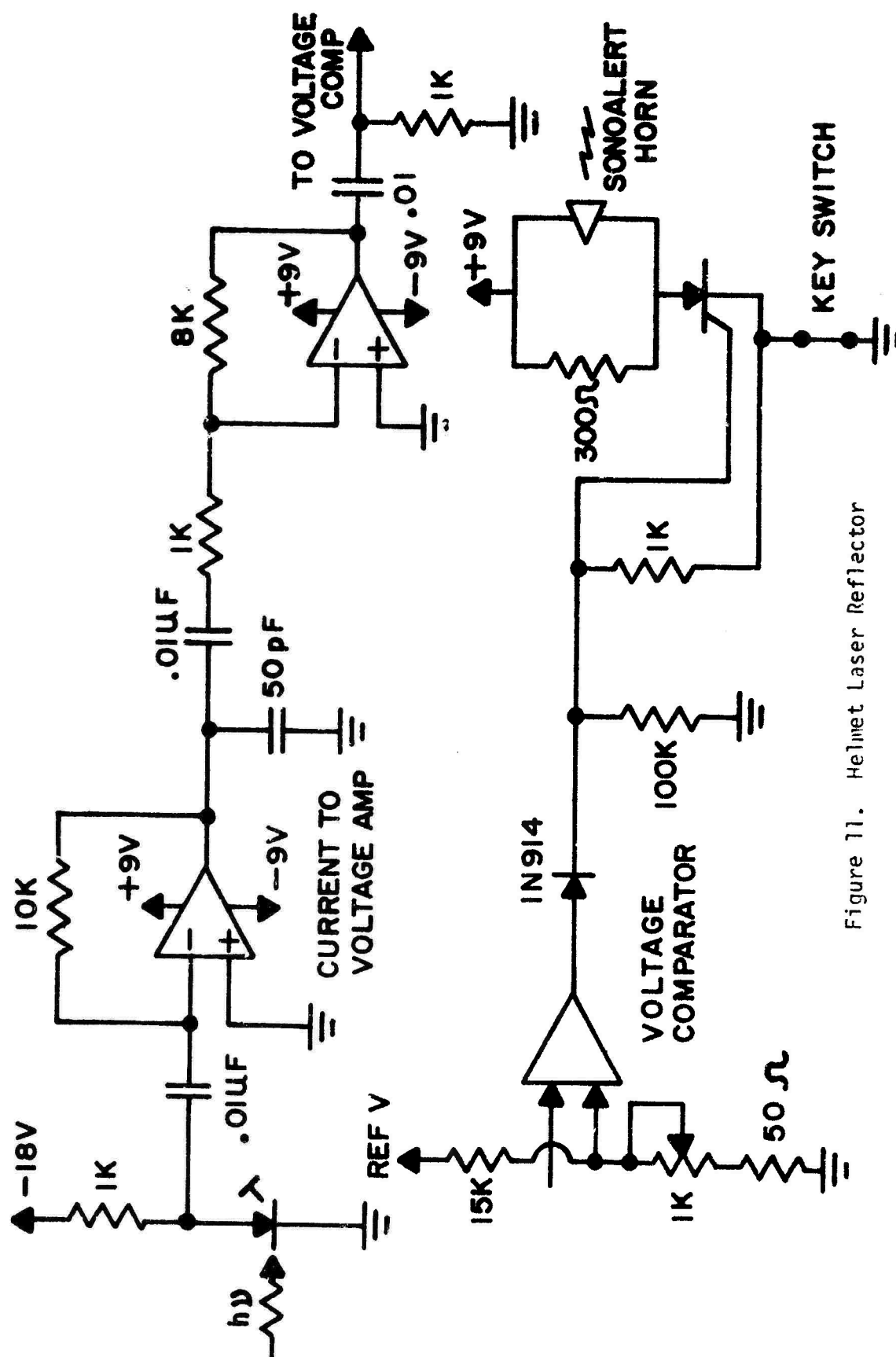


Figure 11. Helmet Laser Reflector

The PIN photodiode is basically a current source with an output impedance which is finite but very large. The current output is amplified by a current-to-voltage converter using an operational amplifier. Operational amplifier current-to-voltage converters present almost zero load impedance to ground because the inverting input appears as a virtual ground. Current from the photodiode flows through the feedback resistor, generating an output voltage.

$$e_{out} = -i_{diode} R_{Feedback}$$

The photodiode utilized has an active area of 1.0 cm^2 and a NEP of $4.0 \times 10^{-13} \text{ W/Hz}^{1/2}$ at 0.9 microns. The operational amplifier used has a $120 \text{ V}/\mu\text{sec}$ slewing rate and a 20 MHz gain-bandwidth product. The operational amplifier is designed for fast transient pulse response.

A minimum bias voltage of greater than four volts is maintained across the photodiode so that it will not saturate in bright sunlight. When the 180 nsec. pulse is received it is coupled to an operational amplifier through a $0.01 \mu\text{F}$ capacitor. The output of the current-to-voltage converter is inverted and further amplified by the second operational amplifier. A high-speed voltage comparator produces a high output voltage when the input pulse exceeds the reference voltage. The reference voltage is set just above the noise level by a potentiometer in the reference level circuit. When the output of the voltage comparator goes high it turns-on a silicon-controlled rectifier used as a switch to control the voltage on an audio alarm (Sono alert). When the key switch on the helmet receiver is closed, the silicon controlled rectifier, SCR, fires upon the application of a gate trigger pulse from the voltage comparator. When the SCR is on, current through the circuit drives a Mallory Sonoalert. The Sonoalert provides an alarm to let a trainee know he has been hit. Switch S1, when opened, will turn off the SCR.

Forward blocking voltage cannot be reapplied until after the minority carrier charge stored in the device as a result of previous forward conduction has been dissipated to a level that can be controlled by the gate bias, otherwise the SCR will self-trigger on again. Even after the SCR has recovered, reapplication of the anode supply voltage may cause self-triggering due to the dv/dt effect. Self-triggering of the SCR due to dv/dt is caused by a capacitive current equal to the product of the anode-gate capacitance of the SCR and the rate of rise (dv/dt) at the applied anode voltage. Effects of dv/dt are controlled by the use of a gate cathode resistor or a current bias. When the key switch is opened the SCR is turned off. After the switch is opened, the anode-gate capacitance charges through the load by-pass resistor and the 100K resistor between gate and ground. When the SCR has recovered, the key switch can be closed, and no capacitive current flows since the anode-gate capacitance is fully charged to the anode voltage. A diode is utilized to decouple the voltage comparator from the SCR when the key switch is opened. The diode prevents the low impedance supply from drawing excessive reverse gate current.

NAVTRAEQUIPCEN IN-227

The detectors worked well without optical filters, however, a glass imbedded gelatin filter such as the 87C may be advisable in long range applications.

SECTION III

CONCLUSIONS AND RECOMMENDATIONS

The prototype system has been successfully demonstrated, and provides a high degree of realism.

It is recommended that a special laser diode be fabricated in the form of a linear diode array, for the kill beam. A single diode will be pulsed when the trigger is squeezed. If a kill is received, the array will be fired giving a large elliptical beam. This arrangement will allow a single laser transmitter, instead of two.

The aiming required by the trainee is quite realistic and the sight picture accurately outlines areas covered with retroreflective material. The retroreflective material is quite durable and the elimination of cables and detectors from the body of the man is deemed to be a significant improvement over other systems.

BIBLIOGRAPHY

1. Yariv, Introduction to Optical Electronics, Holt, Reinehart and Winston, 1971
2. Schiel, E. J., High Gain Silicon Avalanche Detectors, Proceedings at the Electro-Optical Systems Design Conference, 1971
3. Optoelectronics Data Book for Design Engineers, Texas Instruments, Inc.
4. McIntyre, R., Multiplication Noise In Uniform Avalanche Diodes, IEEE Transactions of Electron Devices, Vol. ED-13
5. Electro-Optics Handbook, RCA, Technical Series, EOH-10
6. Kordes, R., Optimize Photodiode Detector Design, Electronic Design, November 9, 1972
7. Baird, J., A Model of the Avalanche Photodiode, IEEE Transactions on Electron Devices, Vol. ED-14, Number 5, May 1967